

Model-Contrastive Learning for Backdoor Defense

Zhihao Yue, Jun Xia, Zhiwei Ling, Ming Hu, Ting Wang, Xian Wei, Mingsong Chen*

¹Shanghai Key Lab of Trustworthy Computing, East China Normal University

*Corresponding Author, {mschen}@sei.ecnu.edu.cn

Abstract

Due to the popularity of Artificial Intelligence (AI) techniques, we are witnessing an increasing number of backdoor injection attacks that are designed to maliciously threaten Deep Neural Networks (DNNs) causing misclassification. Although there exist various defense methods that can effectively erase backdoors from DNNs, they greatly suffer from both high Attack Success Rate (ASR) and a non-negligible loss in Benign Accuracy (BA). Inspired by the observation that a backdoored DNN tends to form a new cluster in its feature spaces for poisoned data, in this paper we propose a novel two-stage backdoor defense method, named MCLDef, based on Model-Contrastive Learning (MCL). In the first stage, our approach performs trigger inversion based on trigger synthesis, where the resultant trigger can be used to generate poisoned data. In the second stage, under the guidance of MCL and our defined positive and negative pairs, MCLDef can purify the backdoored model by pulling the feature representations of poisoned data towards those of their clean data counterparts. Due to the shrunken cluster of poisoned data, the backdoor formed by end-to-end supervised learning is eliminated. Comprehensive experimental results show that, with only 5% of clean data, MCLDef significantly outperforms state-of-the-art defense methods by up to 95.79% reduction in ASR, while in most cases the BA degradation can be controlled within less than 2%. Our code is available at <https://github.com/WeCanShow/MCL>.

1 Introduction

Along with the prosperity of Artificial Intelligence (AI), Deep Neural Networks (DNNs) play a more and more important role in the design of safety-critical systems (e.g., autonomous driving [1], medical diagnosis [2] and plant control [3]) for the purposes of intelligent sensing and control. However, due to the steadily increasing popularity,

DNNs are inevitably becoming the focus of various malicious adversaries [4]. For example, due to biased third-party training data or improper training processes, a tiny adversarial input perturbation during the test phase can fool a target DNN to make misclassification [5], resulting in disastrous consequences. Recently, backdoor attacks [6] have emerged as a notable security threat to DNNs. By poisoning partial training data, adversaries can embed backdoors in some DNN by tricking it to establish the correlations between trigger patterns and target labels. In this way, if some trigger pattern appears at test time, the DNN will make a preset prediction on purpose. In response to the situation of increasing popularity of backdoor attacks, various backdoor defense methods have been developed, which can be mainly classified into two categories. The first one is the detection-based methods [7; 8; 9], which can effectively figure out whether training data are poisoned or training processes are manipulated. However, these methods focus on the detection rather than elimination of triggers within poisoned data or backdoors within DNNs. In this paper, we focus on the second one, i.e., erasing-based methods [10; 11; 12] whose goal is to eliminate the backdoor triggers by purifying the malicious effects of backdoored DNNs.

Although existing erasing-based methods are promising in fixing backdoored DNNs, most of them face with the dilemma that the reduction of Attack Success Rate (ASR) for DNNs may notably sacrifice their Benign Accuracy (BA) on clean data. The reason of such low BA is mainly due to the side effect of purification processes, which messes up the feature space of backdoored DNNs. According to the observation in [13], due to excessive learning capability of the end-to-end supervised learning paradigm, the features of backdoor triggers can be learned. As a result, poisoned data prefer to form a new cluster in the feature space of a backdoored DNN rather than to locate in the ones of benign samples. However, when conducting some kind of purification on the backdoored DNN, the boundaries of benign data clusters become blur, resulting in the low BA. Although the decoupling-based backdoor defense approach introduced in [13] is the first to study backdoors from the perspective of hidden feature space, it focuses on the construction of DNNs that are immune to backdoor attacks rather

than eliminating backdoors from DNNs. When more and more AI applications adopt pre-trained DNNs from untrusted third parties, *how to fully take the advantage of feature distribution characteristics to enhance the capability of erasing backdoor triggers without degrading BA is becoming a challenging direction in backdoor defense.*

Contrastive learning methods [14; 15; 16; 17] have been acknowledged as a promising way to learn better data feature representations. By learning from both positive pairs constructed from different transformations of same samples and negative pairs generated from different samples, contrastive learning can make the features within a positive pair close to each other, and make the two features within a negative pair far away from each other. Therefore, contrastive learning is the best fit for backdoor elimination from the perspective of feature distributions, since it can shrink the cluster of poisoned data as much as possible while making the feature representations close to their benign counterparts. Based on this understanding, in this paper we propose a novel Model-Contrastive Learning (MCL)-based backdoor defense method, named MCLDef, which can make full use of the distribution characteristics of both poisoned and benign samples in the feature space for the purpose of purifying backdoored DNNs. The major contributions of this paper are as follows:

- Based on the distribution characteristics of feature representations, we define both positive pairs and negative pairs for data features that are specific for MCL-based backdoor defense.
- We propose a two-stage MCL framework for backdoor defense, which can effectively shrink or even damage the cluster of poisoned data in the feature space by pulling the feature representations of poisoned data towards to their benign counterparts.
- We conduct experiments against well-known backdoor attacks to show the superiority of MCLDef over state-of-the-art (SOTA) backdoor defense methods in terms of ASR and BA.

The rest of this paper is organized as follows. After the introduction to related work on backdoor inject attack, backdoor defense and contrastive learning in Section 2, Section 3 presents the detail of our MCLDef approach. Section 4 evaluates the effectiveness of our approach against four SOTA backdoor attacks using various well-known benchmarks. Finally, Section 5 concludes the paper.

2 Related Work

Backdoor Attack. Generally, a backdoor attack refers to embedding a backdoor into some DNN by poisoning part of its training data, where triggers can be controlled by adversaries to manipulate DNN outputs, causing incorrect or unexpected behaviors. As the most common backdoor attack paradigm, poisoned-label attacks [6; 18] stamp backdoor triggers onto benign training data and replace their labels with attacker-specified ones. For

example, Chen et al. [19] introduced the *blended attack* that generates poisoned instances and backdoor instances by blending benign input data with a specific key pattern. In practice, to avoid the early detection of backdoor attacks from observable training data, most attackers prefer to adopt backdoor attacks with imperceptible changes, e.g., natural reflection [20] and human imperceptible noise [21]. As an alternative, clean-label attacks only modify partial training data without tempering their labels. For example, Turner et al. [22] proposed the *clean-label attack* that adopts adversarial perturbations or generative models to tamper with benign data from the target class and then performs trigger injection, thus establishing the connection between triggers and their target labels. In [23], Barni et al. implemented a clean-label attack using sinusoidal bands as the trigger. Note that, although clean-label attacks are more stealthy than poisoned-label attacks, they greatly suffers from the problems of low ASR or even failures in creating backdoors [24].

Backdoor Defense. The mainstream backdoor defense methods can be mainly classified into two categories, i.e., the detection-based methods and the erasing-based methods. The former one can be used to: i) identify backdoors of DNNs during the training [7; 25; 26]; or ii) check whether the data are poisoned [8; 27; 28], thus the poisoning data can be safely filtered during the training. The latter category consists of three directions: i) *model reconstruction-based defense* that leverages DNN finetuning [10; 29; 30] using a limited set of clean data to eradicate backdoor triggers; ii) *poison suppression-based defense* that mitigates the impacts of poisoned samples during the training process [11; 13; 31]; and iii) *trigger synthesis-based defense* that uses trigger synthesis to construct poisoned samples for the purpose of backdoor trigger elimination [9; 12].

Contrastive Learning. Contrastive learning has been widely investigated in self-supervised learning to achieve desired feature representations from unlabeled samples [14; 15; 16; 17; 32]. Its basic idea is to reduce the distance of feature representations of two samples within a positive pair as much as possible, and enlarge the distance of feature representations of different samples within negative pairs. Besides the contrastive learning on samples, Model-Contrastive Learning (MCL) has been studied to correct the bias of local models for federated learning [33].

Our approach is inspired by the observation in [13], which has been used to construct DNNs that are immune to backdoor attacks by decoupling training processes. However, this method cannot be directly used to purify backdoored DNNs. To the best of our knowledge, MCLDef is the first attempt that leverages the merits of MCL to eliminate backdoors in DNNs. By correcting the feature representations of poisoned samples, MCLDef can not only mitigate the malicious impacts of backdoor attacks, but also maintain an expected classification performance with high BA.

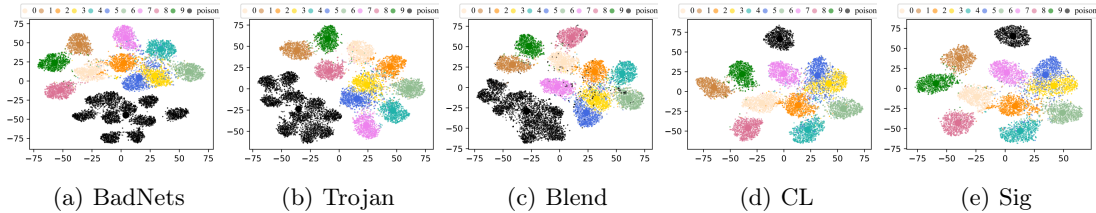


Figure 1: The t-SNE of feature vectors in the hidden feature space under different attacks.

3 Our MCL-based Backdoor Defense Method

In this section, we first show the motivation of our approach from the perspective of feature distributions, and then introduce our two-stage MCL-based backdoor defense method in detail.

Defense Settings. Similar to other classical backdoor defense methods, in this paper we assume that a backdoored DNN is trained by an unreliable third-party dataset, where attackers can arbitrarily modify the training dataset but cannot control the training process. Meanwhile, we assume that partial (e.g., 5%) clean training data is available to finetune the backdoored model. The goal of MCLDef is to use such clean data to purify the poisoned DNN by erasing the injected backdoor without degrading the classification performance on benign data.

3.1 Motivation from Hidden Feature Space

To understand the distribution characteristics of feature representations in the hidden feature space, we evaluate the effects of five backdoor injection attacks, i.e., BadNets [6], Trojan [18], Blend [19], CL [22], and Sig [23], respectively, on Cifar-10 dataset [34]. Here, we obtain feature vectors of the test result from the feature extractor (the DNN without the last classifier layer) and use t-SNE [35] for visualization. Please refer to Appendix A for more details about the experimental settings. Figure 1 shows the distributions of feature representations of both benign and poisoned samples under the five attacks respectively. For different kinds of input training samples, we marked their feature representations in different colors (i.e., color 0 to 9). Note that in each subfigure the feature representations of poisoned data are marked in black color. From this figure, we can clearly find that the feature representations of benign samples from the same category of Cifar-10 form an individual cluster, while all the poisoned samples form a new cluster (in black color) in the feature space. According to the observation in [13], this new cluster implicitly reflects the features of the injected trigger itself. Note that the attacks in Figure 1(a) to 1(c) are all poisoned-label backdoor attacks. From these three subfigures, we can observe that the black cluster can be further divided into 10 subclusters, which correspond to the 10 clusters of their benign counterparts. This phenomenon again demonstrates that the sample feature is also learnt by the DNN. Unlike the three attacks, the ones used in

Figure 1(d) and 1(e) are all clean-label attacks, where we can only find one single dense black cluster for the poisoned samples. This is because clean-label methods only attack the samples with a specific target-label (i.e., the label that corresponds to blue color in this example).

Based on the above observations, we can find that the cluster of poisoned samples indicates the trigger pattern for backdoor attack from the perspective of feature space. In other words, if we can shrink or damage such a cluster of poisoned samples, we can eliminate the backdoor triggers as well. However, this may cause the problem of low BA, since the new features of poisoned samples will be scattered improperly to the incorrect places of the feature space. To avoid BA degradation, it is required that the new features of poisoned samples after purification can be located close to their benign counterparts.

3.2 Overview of Our Approach

In this paper, we resort to MCL for the backdoor defense, which naturally matches the observations in Section 3.1. The basic idea of our approach is to define a benign sample and its poisoned counterpart as a positive pair and define two different benign samples as a negative pair. Under the guidance of MCL, the cluster of poisoned samples will be damaged, and the new features of poisoned samples will be pulled towards to the ones of their benign counterparts. In this way, the backdoor triggers will be eliminated with negligible BA loss.

To enable MCL for backdoor defense, we need to figure out two questions first. The first one is “how can we figure out the clusters for poisoned samples”, and the second one is “how can we accommodate the MCL to enable efficient backdoor defense without degrading BA”. To address these two questions, in this paper we propose a novel two-stage MCL-based backdoor defense method called MCLDef as shown in Figure 2. The first stage performs trigger inversion based on an existing trigger synthesis method presented in [9] that converts the trigger inversion into an optimization problem. Based on the poisoned samples generated by the obtained inverted trigger in the first stage, the second stage utilizes the model-based contrastive learning to purify the backdoored DNNs based on our defined positive and negative pairs. Note that in our approach, we treat a DNN as a combination of two disjoint parts including a feature extractor and a classifier (i.e., fully connected layers), whereas the positive and negative pairs are constructed based on the

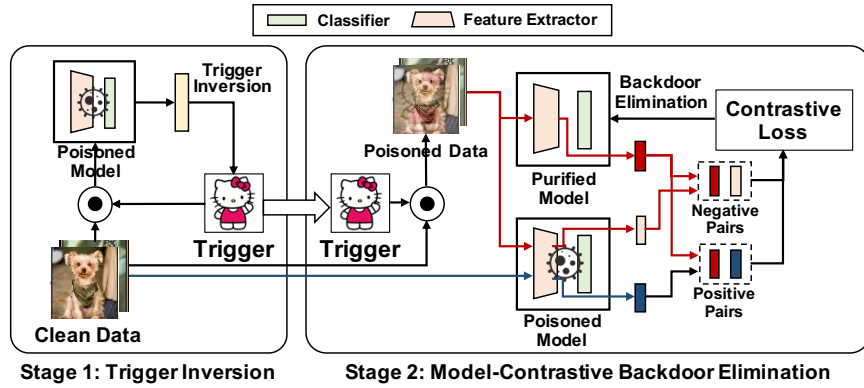


Figure 2: Overview of our MCLDef defense method

outputs of feature extractors of both the poisoned model and purified model. Based on the calculated contrastive loss, the backdoor elimination process iterates until the convergence of purification. The following subsections will detail the key components and steps of our approach.

3.3 Trigger Inversion (Stage 1)

As aforementioned, our approach purifies backdoored DNNs based on both the positive and negative pairs of feature representations. Since our approach only uses a small set of clean samples for the purpose of finetuning, we need to figure out their poisoned counterparts. However, for a given backdoored DNN, it is hard to know which kind of backdoor attack is applied on the model. To address this problem, the first stage of our approach resorts to trigger inversion, which can effectively figure out a trigger to derive poisoned samples with high quality. Here, we adopt the same trigger inversion implementation as the well-known Neural Cleanse (NC) method [9].

Assume that $\mathcal{D} = \{(\mathbf{x}_i, y_i)\}_{i=1}^N$ is a clean dataset, where $\mathbf{x}_i \in \{0, 1, \dots, 255\}^{C \times W \times H}$. We generate the corresponding poisoned dataset $\hat{\mathcal{D}} = \{(\hat{\mathbf{x}}_i, \hat{y}_i)\}_{i=1}^N$ by using the following equation:

$$\hat{\mathbf{x}} = (1 - \mathbf{m}) \odot \mathbf{x} + \mathbf{m} \odot \Delta, \quad (1)$$

where Δ denotes the trigger pattern, $\mathbf{m} \in \{0, 1\}^{W \times H}$ is a binary mask used to determine the trigger position, and \odot indicates the element-wise product. Assuming that the target label be y_t , our approach optimizes the trigger pattern Δ and the mask \mathbf{m} as follows:

$$\Delta^*, \mathbf{m}^* = \arg \min_{\Delta, \mathbf{m}} \sum_{i=1}^N \mathcal{L}(f(\hat{\mathbf{x}}_i; \bar{\omega}), y_t) + \lambda |\mathbf{m}|, \quad (2)$$

where $\bar{\omega}$ is the poisoned model parameters. $f(\cdot)$ is the DNN output, $\mathcal{L}(\cdot)$ is the cross-entropy loss function, and λ is a hyperparameter that controls the weight of the regularization. Here, we assume that the target label of backdoor attacks has been detected by some method, e.g., the ones proposed in [7; 9; 25]. Based on Equation 2, we can obtain an optimized trigger pattern Δ^* and its mask \mathbf{m}^* .

3.4 Construction of Positive and Negative Pairs

The positive pairs and negative pairs play an important role in MCL to determine the correlations between feature representations in feature space. By definition, after the contrastive learning, the two elements of a positive pair will become closer to each other, while the distance of two elements within a negative pair will become longer. Based on these facts, to accommodate MCL to the backdoor defense, we define the positive pairs by coupling the feature representation of a benign sample in the poisoned model and the feature representation of its poisoned counterpart from the purified model together. Since the poisoned model behaves normally on benign samples, in this way we can pull the feature representations of poisoned samples toward those of their clean sample counterparts in the feature space of purified model, thus the BA can be guaranteed. Meanwhile, since we want to shrink or even totally damage the cluster of poisoned samples in the purified model, we define a negative pair by coupling the feature representations of a poisoned sample in both the poisoned model and purified model together. In this way, the purification can scatter the clustered feature representations of poisoned samples within feature space of the purified model, thus damaging the trigger pattern of the purified model.

Formally, for a given benign sample $(\mathbf{x}, y) \in \mathcal{D}$, we can get the corresponding poisoned sample $(\hat{\mathbf{x}}, \hat{y}) \in \hat{\mathcal{D}}$ by Equation 1. Let $h(\cdot)$ denote the feature vector output by the feature extractor (represented by the pink trapezoid in Figure 2). Let ω and $\bar{\omega}$ denote the parameters of purified DNN and poisoned DNN, respectively, where $\omega = \bar{\omega}$ at the beginning of the second stage. Assuming that $\mathbf{z} = h(\hat{\mathbf{x}}; \omega)$, $\mathbf{z}^{poi} = h(\hat{\mathbf{x}}; \bar{\omega})$, and $\mathbf{z}^{cle} = h(\mathbf{x}; \bar{\omega})$, we can construct a positive pair using $(\mathbf{z}, \mathbf{z}^{cle})$ and a negative pair using $(\mathbf{z}, \mathbf{z}^{poi})$.

3.5 MCL-based Backdoor Elimination (Stage 2)

As aforementioned, we can get the trigger pattern and the mask, which can be used to generate the poisoned

data. According to the definition of positive and negative pairs in Section 3.4, we can get the positive pairs and negative pairs. However, the final goal is to eliminate the backdoor trigger and reduce the loss of the BA. Therefore, we need to accommodate the MCL to enable efficient backdoor defense without degrading BA. The second stage of our approach resorts to MCL, which can reduce the distance of feature representations of a positive pair as much as possible, while enlarging the distance of feature representations of a negative pair.

Figure 2 present the detailed structure of stage 2 in its right part. Once stage 1 finishes, we can obtain an optimized trigger pattern Δ^* and its mask m^* from Equation 2. Assume that \mathcal{D} is a clean dataset with N clean samples and the derived trigger (i.e., the combination of Δ^* and m^*). Based on these two things, we can generate a set of N poisoned samples using Equation 1, denoted as $\hat{\mathcal{D}}$. Let (\mathbf{x}_i, y_i) be a clean sample and $(\hat{\mathbf{x}}_i, \hat{y}_i)$ be its corresponding poisoned sample. According to the definition of positive and negative pairs in Section 3.4, we can generate the corresponding positive pair $(\mathbf{z}_i, \mathbf{z}_i^{cle})$ and negative pair $(\mathbf{z}_i, \mathbf{z}_i^{poi})$ for \mathbf{x}_i and $\hat{\mathbf{x}}_i$. Based on the NT-Xent loss function [36] that is commonly used as a template in contrastive learning and our proposed positive and negative pairs, we define our model-contrastive loss for MCLDef as follows:

$$\mathcal{L}_{contrastive} = \sum_{i=1}^N -\log \frac{\exp(\text{sim}(\mathbf{z}_i, \mathbf{z}_i^{cle})/\tau)}{\exp(\text{sim}(\mathbf{z}_i, \mathbf{z}_i^{cle})/\tau) + \exp(\text{sim}(\mathbf{z}_i, \mathbf{z}_i^{poi})/\tau)}, \quad (3)$$

where τ is a temperature parameter that controls the smoothness of soft labels, and $\text{sim}(\cdot, \cdot)$ represents the similarity of two feature vectors based on the cosine similarity function. In stage 2, we optimize ω via MCL as follows:

$$\omega^* = \arg \min_{\omega} \mathcal{L}_{contrastive}. \quad (4)$$

4 Experiments

To show the effectiveness of our approach, we implemented MCLDef using Pytorch, and compared the performance of MCLDef with four start-of-the-art (SOTA) backdoor elimination methods. All the experimental results were obtained from a workstation with 3.6GHz Intel i9 CPU, 32GB memory, NVIDIA GeForce RTX3090 GPU, and Ubuntu operating system. We designed comprehensive experiments to answer the following three research questions:

RQ1 (Superiority over SOTA): What are the advantages of MCLDef compared with SOTA methods?

RQ2 (Effectiveness of MCL): Can MCL improve the defense performance of purified DNNs?

RQ3 (Applicability of MCLDef): What are the factors (e.g., clean data rates, trigger inversion quality) that greatly impact the performance of MCLDef?

4.1 Experimental Settings

Datasets and DNNs. We evaluated all the defense methods on three classical benchmark datasets, i.e., Cifar-10 [34], GTSRB [37], and an ImageNet subset (with first

20 categories) [38]. We used WideResNet(WRN-16-1) [39] and ResNet18 [40] as the DNNs for the experiments. The statistics of datasets and DNNs adopted in the experiments are presented in Table 3 (see Appendix B.1).

Attack Configurations. We evaluated the performance of five attacks including four SOTA methods, which can be classified into two categories: i) poisoned-label attacks including BadNets [6], Trojan [18], and Blend [19], where the poisoning data rate is 10% and the target label is $y_t = 5$; and ii) clean-label attacks including CL [22] and Sig [23], where the poisoning data rate is 8% and the target label is $y_t = 5$. We followed the settings suggested by [10] to configure these attacks. Please see Appendix B.2 for more details.

Defense Configurations. We compared MCLDef with four SOTA backdoor defense methods, i.e., Fine-Tuning (FT) [18], Neural Attention Distillation (NAD) [10], Implicit Backdoor Adversarial Unlearning (I-BAU) [30], and Neural Cleanse (NC) with unlearning strategy [9]. Similar to the work in [10], we assumed that all the methods could access 5% clean training data for the finetuning. For MCLDef, we adopted the same settings as the ones used by NC [9] for the implementation of trigger inversion. Note that the initial purified model and poisoned model in model-contrastive backdoor elimination are the same. For the purified model, we set its SGD optimizer with a momentum of 0.9, a weight decay of 1×10^{-4} , and an initial learning rate of 0.1 on both Cifar-10 and the ImageNet subset (0.01 on GTSRB). We used a batch size of 64 and finetuned the model for 20 epochs. For the contrastive loss, we set $\tau = 0.5$. For fair comparison, the settings of other four defense methods are consistent with MCLDef. Please see Appendix B.3 for more implementation details.

Evaluation Metrics. Based on the clean test dataset, we used two metrics to evaluate the performance of all the defense methods: i) Attack Success Rate (ASR) indicating the ratio of succeed attacks over all the attacks on clean test samples without target labels; and ii) Benign Accuracy (BA) denoting the ratio of correctly classified samples over all the clean samples.

4.2 Comparison with SOTA Defense Methods (RQ1)

Table 1 compares the performance of MCLDef with the ones of the four SOTA defense methods against five well-known attack methods. Here, we use *Before* to indicate the method with no defense. Note that to enhance the defense performance, here we adopt the data augmentation techniques for backdoor trigger elimination for all the defense methods. Please refer to Appendix C.1 for more results about the impacts of data augmentation.

From this table, we can find that for the dataset Cifar-10, MCLDef achieves the best ASR among all the five defense methods. and the best BA in four out of five attacks. Specifically, compared with the second-best results marked with underscores, MCLDef can reduce the ASR by 21.27%, 32.12%, 8.22%, 95.79%, and 47.72% for the five defense methods, respectively. For the Sig

Table 1: Performance comparison between MCLDef and four SOTA defense methods

Dataset	Attack	Before		FT		NAD		I-BAU		NC		MCLDef	
		ASR	BA	ASR	BA	ASR	BA	ASR	BA	ASR	BA	ASR	BA
Cifar-10	BadNets	99.64	83.01	12.78	80.64	5.76	81.71	2.82	79.54	3.58	81.37	2.22	82.19
	Trojan	99.38	82.84	17.13	80.93	5.14	81.20	5.36	80.05	3.86	79.61	2.62	82.04
	Blend	98.98	84.20	2.51	80.12	3.84	80.79	2.31	81.54	3.01	80.94	2.12	83.98
	CL	95.47	86.44	6.7	80.34	6.99	81.39	13.62	82.15	5.71	77.31	0.24	83.97
	Sig	99.03	84.64	68.17	80.98	6.81	81.79	72.51	80.51	17.33	73.34	3.56	73.81
GTSRB	BadNets	100	97.86	13.25	92.04	4.85	92.89	1.79	91.55	0.68	92.31	0.92	96.32
	Trojan	99.38	98.08	20.99	92.13	8.54	91.94	23.73	90.12	0.54	92.37	2.77	96.41
	Blend	99.04	97.79	10.63	93.13	9.62	93.01	28.62	90.58	1.08	91.39	0.32	96.22
ImageNet	BadNets	100	79.16	2.21	71.26	4.84	72.74	4.1	41.37	0.84	72.42	1.79	79.89
	Trojan	98.21	82.53	2.74	70.84	1.05	74.21	3.16	35.16	1.26	74.32	0.84	83.37
	Blend	99.26	84.32	18.11	75.37	14.32	74.32	1.36	29.58	5.89	68.84	3.58	81.89

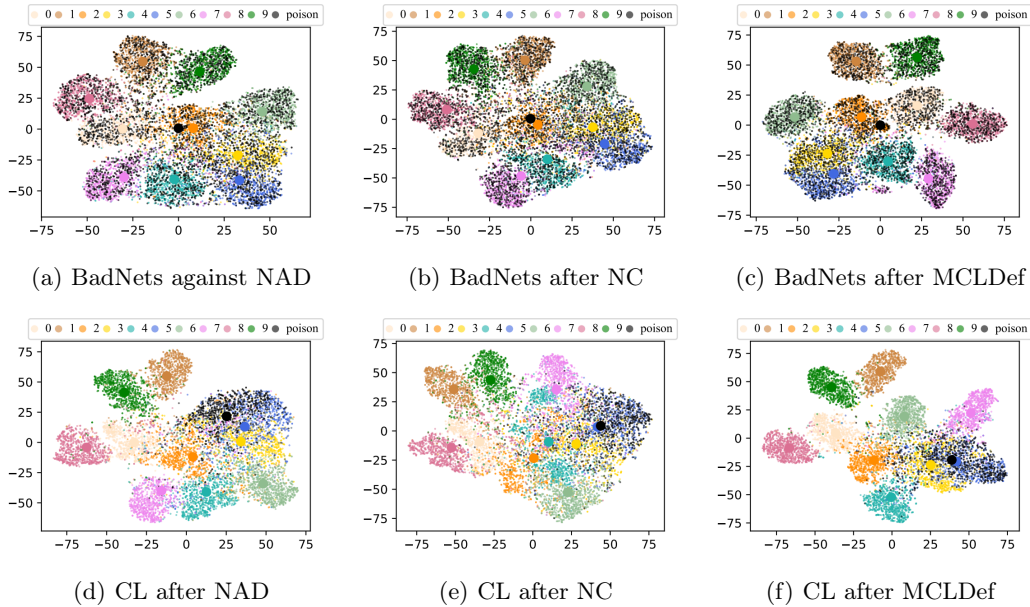


Figure 3: The t-SNE of the feature representations under different attacks after defenses.

attack, the reason of low BA for MCLDef (i.e., 73.81%) is mainly due to the bad quality of trigger inversion, which is also reflected in the case of NC (i.e., 73.34%). Note that the datasets GTSRB and ImageNet often cause the failures for clean-label attacks, we do not provide their comparison results here. We can observe that, for the datasets GTSRB and ImageNet, MCLDef can achieve the best BA and top-2 best ASR for all the cases. As an example for GTSRB with Blend attack, MCLDef outperforms NC by up to 70.37% in ASR, and outperforms FT by 3.3% in BA.

4.3 Effects of MCL on Feature Space (RQ2)

To show the reason why MCLDef outperforms other defense methods, we investigate the feature distributions in feature space. Due to the space limitation, we only provide the results for the two representatives (i.e., Bad-

Nets and CL) of poisoned-label attacks and clean-label attacks.

Based on Cifar-10, Figure 3 visualizes the distributions in feature space for the two representative attacks, where each backdoored DNN is purified by three defense methods (i.e., NAD, NC and MCLDef). Note that, unlike the Figure 1 that only uses the training data for t-SNE visualization, all the six subfigures in Figure 3 show the t-SNE using both training data and extra 5% clean data for purification. From Figure 3(a) to 3(c), we can find that the clusters of poisoned samples in different subfigures are all damaged by the three defense methods, respectively. However, in Figure 3(c) there are fewer black features locating outside the clusters than the other two subfigures, indicating that MCLDef can achieve better BA after defending BadNets attacks. Similarly, in 3(d) to 3(f) the cluster of poisoned samples by CL is also damaged. Since CL is a clean-label attack that focuses on the attacking

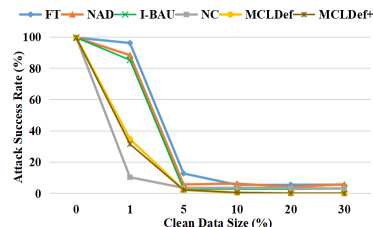
Table 2: Defense performance comparison of different trigger inversion-based methods on Cifar-10.

Attack	Before		NC		MCLDef		MESA		MCLDef(True)	
	ASR	BA	ASR	BA	ASR	BA	ASR	BA	ASR	BA
BadNets	99.64	83.01	3.58	81.37	2.22	82.19	1.34	82.76	0.66	83.24
Trojan	99.38	82.84	3.86	79.61	2.62	82.04	1.50	82.76	0.37	83.43
Blend	98.98	84.20	3.01	80.94	2.12	83.98	/	/	1.16	83.97
CL	95.47	86.44	5.71	77.31	0.24	83.97	0.09	84.98	0.02	85.24
Sig	99.03	84.64	17.33	73.34	3.56	73.74	/	/	0	81.92

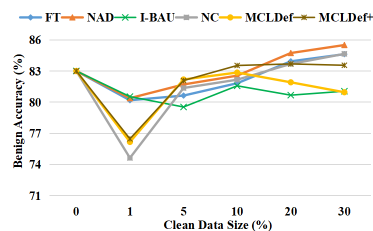
samples with a specific target label (indicated by the blue color here), we can find that the black features locate in the blue cluster in a more concentrated manner, thus leading to a better BA.

4.4 Applicability Analysis (RQ3)

Impact of Clean Data Sizes. Based on dataset Cifar-10, Figure 4 shows the defense performance trends of five defense methods (FT, NAD, I-BAU, NC, MCLDef) against BadNets attack with different sizes of clean data. Please refer to Appendix C.3 for more results of other four backdoor attacks. From this figure, we can find that more clean data will lead to lower ASR and higher BA for the purified DNNs of all the defense methods. Note that with only 1% clean data, both NC and MCLDef can achieve significant ASR reduction, while ASR improvements of the other three defense methods are negligible. However, in this case both NC and MCLDef need to sacrifice their BA, since the the quality of trigger inversion is poor due to a limited number of clean data. When the clean data rate is in between the range [5%, 10%] we can find that ASRs of the five attacks will not change notably, and MCLDef can achieve the best ASR and BA. When the clean data rate reaches 20%, although MCLDef has the best ASR, its BA drops. Note that in this case the BA of FT, NAD, and NC becomes higher than the BA (i.e., 83.01%) of the method without defense. The main reason of the decreasing trend of BA is because MCLDef is based on MCL, where the distance between two features within a negative becomes farther along the backdoor purification process. When more and more clean data are involved in backdoor trigger elimination, such mutual exclusion between features imposed by negative pairs will more easily result in the shape change of benign clusters, leading to lower BA. To verify the reason of this phenomenon, we developed a new method MCLDef+ with one more stage than MCLDef, where the third stage only uses the positive pairs to eliminate the backdoor from the purified model generated by stage two. The goal of the third stage is to increase BA by further pulling the features in positive pairs closer to their corresponding benign clusters. Please see Figure 8 in Appendix C.2 for more details about MCLDef+. From Figure 4(b), we can find that when more clean data are provided, MCLDef+ can achieve better BA than MCLDef. Note that if the size of available clean data is small (i.e., clean sample rate is less than 10%), we suggest to use MCLDef. Otherwise, MCLDef+ is a better choice for backdoor defense.



(a) ASR (against BadNets)



(b) BA (against BadNets)

Figure 4: The defense performance against BadNets with different clean data sizes on Cifar-10.

Influence of Trigger Inversion Quality. To understand the impact of trigger inversion quality on MCLDef, we investigated various trigger inversion methods, which are used to replace the first stage of our approach. For example, we tried to use Max-Entropy Staircase Approximator (MESA) [12] as an alternative (with $\alpha = 0.1$ and $\beta = 0.8$) to replace our trigger inversion part in the first stage. Since MESA makes a stronger assumption that both the size and location of a trigger is known a priori, its trigger inversion quality is better than ours. Note that due to limitations specific in MESA, we only implemented the MESA-based defense against three attacks excluding Blend and Sig attacks. Moreover, instead of using trigger inversion, we developed a method named *MCLDef(True)*, where the first stage is replaced with a hard-coded real trigger with the highest trigger inversion capability among all the methods. Table 2 compares the performance of all the trigger-inversion based methods. From this table, we can find that the higher quality the trigger inversion method has, the better ASR and BA the corresponding defense can achieve.

5 Conclusion

Inspired by the observation that in the feature space of a backdoored DNN the feature representations of both

benign samples with the same category and the poisoned samples are separately clustered, we proposed a novel two-stage model-contrastive learning framework named MCLDef for the purpose of backdoor defense. Based on our proposed definitions of positive and negative pairs of features, MCLDef can shrink or even damage the cluster of poisoned samples and pull the poisoned samples towards the clusters of their benign counterparts. In this way, the backdoor triggers in DNNs are eliminated and the classification accuracy on benign samples can be guaranteed. Comprehensive experimental results shows that, compared with various kinds of state-of-the-art defense methods, our approach can not only achieve significantly lower ASR but also have a better benign accuracy under the help of only 5% clean data.

References

- [1] Yue Wang, Alireza Fathi, Abhijit Kundu, David A Ross, Caroline Pantofaru, Tom Funkhouser, and Justin Solomon. Pillar-based object detection for autonomous driving. In *ECCV*, pages 18–34, 2020.
- [2] Xiaosong Wang, Yifan Peng, Le Lu, Zhiyong Lu, Mohammadhadi Bagheri, and Ronald M. Summers. Chestx-ray8: Hospital-scale chest x-ray database and benchmarks on weakly-supervised classification and localization of common thorax diseases. In *CVPR*, pages 3462–3471, 2017.
- [3] Yong Shi, Xiaodong Xue, Jiayu Xue, and Yi Qu. Fault detection in nuclear power plants using deep learning based image classification with imaged time-series data. *Int. J. Comput. Commun. Control*, 17(1), 2022.
- [4] Yunfei Song, Tian Liu, Tongquan Wei, Xiangfeng Wang, Zhe Tao, and Mingsong Chen. FDA³: Federated defense against adversarial attacks for cloud-based iiot applications. *IEEE TII*, 17(11):7830–7838, 2021.
- [5] Nicholas Carlini and David A. Wagner. Towards evaluating the robustness of neural networks. In *S&P*, pages 39–57, 2017.
- [6] Tianyu Gu, Kang Liu, Brendan Dolan-Gavitt, and Siddharth Garg. Badnets: Evaluating backdoor-attacking attacks on deep neural networks. *IEEE Access*, 7:47230–47244, 2019.
- [7] Songzhu Zheng, Yikai Zhang, Hubert Wagner, Mayank Goswami, and Chao Chen. Topological detection of trojaned neural networks. In *NeurIPS*, pages 17258–17272, 2021.
- [8] Jonathan Hayase and Weihao Kong. Spectre: Defending against backdoor attacks using robust covariance estimation. In *ICML*, 2021.
- [9] Bolun Wang, Yuanshun Yao, Shawn Shan, Huiying Li, Bimal Viswanath, Haitao Zheng, and Ben Y Zhao. Neural cleanse: Identifying and mitigating backdoor attacks in neural networks. In *S&P*, pages 707–723, 2019.
- [10] Yige Li, Xixiang Lyu, Nodens Koren, Lingjuan Lyu, Bo Li, and Xingjun Ma. Neural attention distillation: Erasing backdoor triggers from deep neural networks. In *ICLR*, 2021.
- [11] Yige Li, Xixiang Lyu, Nodens Koren, Lingjuan Lyu, Bo Li, and Xingjun Ma. Anti-backdoor learning: Training clean models on poisoned data. In *NeurIPS*, pages 14900–14912, 2021.
- [12] Ximing Qiao, Yukun Yang, and Hai Li. Defending neural backdoors via generative distribution modeling. In *NeurIPS*, pages 14004–14013, 2019.
- [13] Huang Kunzhe, Li Yiming, Wu Baoyuan, Qin Zhan, and Ren Kui. Backdoor defense via decoupling the training process. In *ICLR*, 2022.
- [14] Ting Chen, Simon Kornblith, Mohammad Norouzi, and Geoffrey Hinton. A simple framework for contrastive learning of visual representations. In *ICML*, 2020.
- [15] Ting Chen, Simon Kornblith, Kevin Swersky, Mohammad Norouzi, and Geoffrey E Hinton. Big self-supervised models are strong semi-supervised learners. In *NeurIPS*, pages 22243–22255, 2020.
- [16] Kaiming He, Haoqi Fan, Yuxin Wu, Saining Xie, and Ross Girshick. Momentum contrast for unsupervised visual representation learning. In *CVPR*, pages 9726–9735, 2020.
- [17] Xinlei Chen and Kaiming He. Exploring simple siamese representation learning. In *CVPR*, pages 15750–15758, 2021.
- [18] Yingqi Liu, Shiqing Ma, Yousra Aafer, Wenchuan Lee, Juan Zhai, Weihang Wang, and Xiangyu Zhang. Trojaning attack on neural networks. In *NDSS*, 2018.
- [19] Xinyun Chen, Chang Liu, Bo Li, Kimberly Lu, and Dawn Song. Targeted backdoor attacks on deep learning systems using data poisoning. *arXiv preprint arXiv:1712.05526*, 2017.
- [20] Yunfei Liu, Xingjun Ma, James Bailey, and Feng Lu. Reflection backdoor: A natural backdoor attack on deep neural networks. In *ECCV*, pages 182–199, 2020.
- [21] Haoti Zhong, Cong Liao, Anna Cinzia Squicciarini, Sencun Zhu, and David Miller. Backdoor embedding in convolutional neural network models via invisible perturbation. In *CODASPY*, pages 97–108, 2020.
- [22] Alexander Turner, Dimitris Tsipras, and Aleksander Madry. Label-consistent backdoor attacks. *arXiv preprint arXiv:1912.02771*, 2019.
- [23] Mauro Barni, Kassem Kallas, and Benedetta Tondi. A new backdoor attack in CNNs by training set corruption without label poisoning. In *ICIP*, pages 101–105, 2019.
- [24] Yiming Li, Baoyuan Wu, Yong Jiang, Zhifeng Li, and Shutao Xia. Backdoor learning: A survey. *arXiv preprint arXiv:2007.08745*, 2020.

- [25] Yinpeng Dong, Xiao Yang, Zhijie Deng, Tianyu Pang, Zihao Xiao, Hang Su, and Jun Zhu. Black-box detection of backdoor attacks with limited information and data. In *ICCV*, pages 16462–16471, 2021.
- [26] Zhen Xiang, David J Miller, and George Kesidis. Post-training detection of backdoor attacks for two-class and multi-attack scenarios. In *ICLR*, 2022.
- [27] Yi Zeng, Won Park, Z Morley Mao, and Ruoxi Jia. Rethinking the backdoor attacks’ triggers: A frequency perspective. In *ICCV*, pages 16453–16461, 2021.
- [28] Di Tang, XiaoFeng Wang, Haixu Tang, and Kehuan Zhang. Demon in the variant: Statistical analysis of dnns for robust backdoor contamination detection. In *USENIX Security*, pages 1541–1558, 2021.
- [29] Kang Liu, Brendan Dolan-Gavitt, and Siddharth Garg. Fine-pruning: Defending against backdooring attacks on deep neural networks. In *RAID*, pages 273–294, 2018.
- [30] Yi Zeng, Si Chen, Won Park, Z Morley Mao, Ming Jin, and Ruoxi Jia. Adversarial unlearning of backdoors via implicit hypergradient. In *ICLR*, 2022.
- [31] Eitan Borgnia, Valeriia Cherepanova, Liam Fowl, Amin Ghiasi, Jonas Geiping, Micah Goldblum, Tom Goldstein, and Arjun Gupta. Strong data augmentation sanitizes poisoning and backdoor attacks without an accuracy tradeoff. In *ICASSP*, pages 3855–3859, 2021.
- [32] Longlong Jing and Yingli Tian. Self-supervised visual feature learning with deep neural networks: A survey. *IEEE TPAMI*, 43(11):4037–4058, 2021.
- [33] Qinbin Li, Bingsheng He, and Dawn Song. Model-contrastive federated learning. In *CVPR*, pages 10713–10722, 2021.
- [34] Alex Krizhevsky, Geoffrey Hinton, et al. Learning multiple layers of features from tiny images. In *Citeseer*, 2009.
- [35] Laurens Van der Maaten and Geoffrey Hinton. Visualizing data using t-SNE. *Journal of machine learning research*, 9(11), 2008.
- [36] Kihyuk Sohn. Improved deep metric learning with multi-class n-pair loss objective. In *NeurIPS*, pages 1849–1857, 2016.
- [37] Johannes Stalkamp, Marc Schlipf, Jan Salmen, and Christian Igel. Man vs. computer: Benchmarking machine learning algorithms for traffic sign recognition. *Neural networks*, 32:323–332, 2012.
- [38] Jia Deng, Wei Dong, Richard Socher, Li-Jia Li, Kai Li, and Li Fei-Fei. Imagenet: A large-scale hierarchical image database. In *CVPR*, pages 248–255, 2009.
- [39] Sergey Zagoruyko and Nikos Komodakis. Wide residual networks. In *BMVC*, 2016.
- [40] Kaiming He, Xiangyu Zhang, Shaoqing Ren, and Jian Sun. Deep residual learning for image recognition. In *CVPR*, pages 770–778, 2016.
- [41] Paulius Micikevicius, Sharan Narang, Jonah Alben, Gregory Diamos, Erich Elsen, David Garcia, Boris Ginsburg, Michael Houston, Oleksii Kuchaiev, Ganesh Venkatesh, et al. Mixed precision training. In *ICLR*, 2018.

A Implementation Details for Section 3.1

Attack Settings. We evaluated the effects of five backdoor injection attacks on the Cifar-10 dataset, which can be classified into two categories: i) poisoned-label attacks including BadNets [6], Trojan [18], Blend [19], where the poisoned data rate is 10% and the target label is $y_t = 5$; and ii) clean-label attacks including CL [22], Sig [23], where the poisoned data rate is 8% and the target label is $y_t = 5$. For BadNets, we used the grid trigger with a size of 3×3 placed in the bottom right corner of the image. For Trojan, we used a 3×3 trigger placed in the bottom right corner of the image. For Blend, to better reflect the advantages of our defense method, we used a random color trigger with a size of 3×3 placed in the center of the image, and the blend rate was set to 0.1. For CL, we followed the same settings as used in [22], where we used the Projected Gradient Descent (PGD) [41] under the l_∞ norm with a maximum perturbation size $\epsilon = 8$ to generate adversarial perturbed data, and adopted a grid trigger with a size of 3×3 placed in the bottom right corner of the image. For Sig, we generated the trigger by following the horizontal sine function as defined in [23], where $\Delta = 20$ and $f = 6$. Figure 5 gives the examples generated by the five backdoor attacks in our experiments.

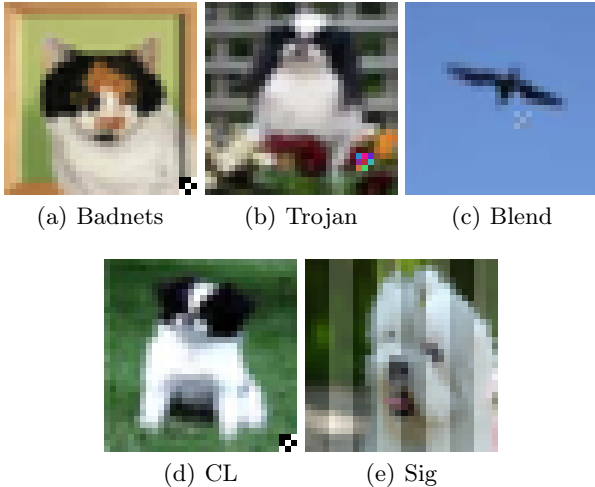


Figure 5: Examples of backdoored Cifar-10 images by five different attacks.

Training Setting. To train a poisoned model on Cifar-10 for the examples shown in Figure 1, we set its SGD optimizer with a momentum of 0.9, a weight decay of 1×10^{-4} , and an initial learning rate of 0.1. With a batch size of 64, we trained the WRN-16-1 network for 50 epochs. Note that at the 20th and the 35th epoch, the learning rate will be reduced by a factor of 10, respectively. To avoid side effects of backdoor attacks, we did not use any data augmentation techniques.

t-SNE Visualization Setting. To observe the dis-

tribution characteristics of both benign and poisoned samples in feature space, we used different colors in t-SNE visualization for benign samples with a specific category and poisoned samples, respectively. Here, we use the feature vectors obtained from the feature extractor (a DNN without the last layer of classifiers) as the inputs of t-SNE [35] for visualization. To enable better visualization effect, all the t-SNE figures in this paper show all the investigated poisoned samples and partial (i.e., 20%) clean samples that are randomly selected from each category of a dataset.

B Implementation Details for Section 4

B.1 Settings of Datasets and DNNs

Table 3 presents the statistics of datasets and DNNs used in our experiments.

B.2 Settings of Attacks

Attack Details. We applied five backdoor injection attacks on the Cifar-10 dataset [34], which can be classified into two categories: i) poisoned-label attacks including BadNets [6], Trojan [18], Blend [19], where the poisoning data rate is 10% and the target label is $y_t = 5$; and ii) clean-label attacks including CL [22], Sig [23]. The attack settings for Cifar-10 are the same as the ones described in Appendix A. Note that we only performed the poisoned-label backdoor attacks (i.e., BadNets, Trojan, and Blend) on GTSRB dataset [37]. We imposed the triggers on GTSRB images in a same way as the one used in Cifar-10 as described in Section A. Figure 6 presents three examples of backdoored GTSRB images. We only conducted the poisoned-label backdoor attacks on the ImageNet subset [38], where the poisoned data rate is 10% and the target label is $y_t = 5$. For BadNets and Trojan attacks on ImageNet images, we injected a grid trigger with a size of 32×32 in the bottom right corner of the image. For Blend attacks, we applied the ‘‘Hello Kitty’’ trigger on ImageNet images. Figure 7 presents three examples of backdoored ImageNet images.

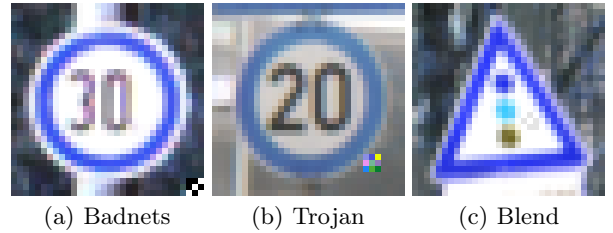
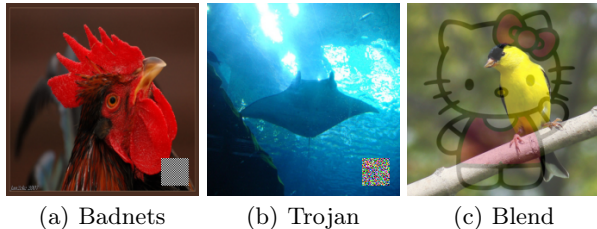


Figure 6: Examples of backdoored GTSRB images by three different attacks.

Training Settings. For datasets Cifar10 and GTSRB, we used the same training settings as those described in Appendix A. Note that for GTSRB, we set the initial learning rate of the optimizer to 0.01. For the ImageNet subset, we trained the Resnet-18 network for 100 epochs with a batch size of 32, where the learning rate was

Table 3: Statistics of datasets

Dataset	Input Size	Classes	Training Images	Test Images	DNN model
Cifar-10	$3 \times 32 \times 32$	10	50000	10000	WideResNet-16-1
GTSRB	$3 \times 32 \times 32$	43	26640	12569	WideResNet-16-1
ImageNet subset	$3 \times 224 \times 224$	20	26000	1000	ResNet-18



(a) Badnets (b) Trojan (c) Blend

Figure 7: Examples of backdoored ImageNet images by three different attacks.

reduced by a factor of 10 at the 20th and the 70th epoch, respectively. To enhance the generalization of target DNNs, we used various data augmentation techniques, e.g., random crop and random horizontal flipping. All the other settings are the same as those applied on Cifar-10.

B.3 Settings of Defenses

For the purpose of trigger inversion, in MCLDef and NC we optimized the trigger pattern and mask using the Adam optimizer with a momentum of 0.9, and a learning rate of 0.005. The optimization involves 100 epochs with a batch size of 64. For datasets Cifar-10 and GTSRB, we set λ of the optimization objective to 0.01. For the ImageNet subset, we set $\lambda = 0.001$.

For the backdoor elimination purpose, we finetuned all the backdoored model (e.g., the purified model in MCLDef) for 20 epochs for all the five defense methods, where the learning rate was reduced by a factor of 10 at both the 2nd and 10th epochs. Note that to enhance the defense quality, we used data augmentation techniques (including random crop and random horizontal flipping) for finetuning. For NAD, when dealing with datasets Cifar-10 and GTSRB, we use the same setting as described in [10]. When dealing with the ImageNet subset, we calculated the NAD loss only based on the last three residual groups of ResNet-18. To achieve a best trade-off between ASR and BA, we set $\beta = 5000$. Since the settings of MCLDef used in this paper are not suitable for I-BAU, in the experiment I-BAU used the settings as described in [11].

Based on the above defense settings, we implemented the defense methods FT and NAD by modifying the source code of NAD¹. We adopted NC based on the open source code from its official website². By slightly modifying the part of dataset loading and model loading, we implemented I-BAU based on the open-source code from its

official website³.

C Supplementary Experimental Results

In this section, we provide more experiments to show the advantages of MCLDef, whose code is available at <https://github.com/WeCanShow/MCL>.

C.1 Impact of Data Augmentation Techniques

To investigate the impact of data augmentation, here we considered two cases: i) data augmentation is not used in backdoor trigger elimination; and ii) data augmentation is used in the training of poisoned model. Here, we only consider two kinds of data augmentation techniques, random crop and random horizontal flipping.

Defense without Data Augmentation. Table 4 shows the defense performance without using data augmentation techniques for the five defense methods by using Cifar-10 dataset. From this table, we can find that our MCLDef can achieve the best performance in ASR, and the best BA in three out of five attacks. The difference between the defense performance of MCLDef in Table 1 and Table 4 is negligible. Note that, we can find that FT and NAD methods greatly rely on the use of data augmentation techniques. Compared with the results in Table 1, the ASR of NAD against Trojan is 91.08% without considering data augmentation, while the ASR of NAD against Trojan is 5.14% by taking the data augmentation into account.

Attack with Data Augmentation. To enhance the attack performance, data augmentation techniques are widely used in the training of poisoned models. To evaluate the performance of MCLDef for this case, we use the data augmentation techniques (i.e., random crop and random horizontal flipping) to derive training samples for poisoned models. To accommodate such extra training samples, in CL attack we changed the position of triggers accordingly, i.e., we placed the trigger in the center of images. To obtain the poisoned models for the five attacks, we trained each backdoored DNN for 100 epochs with an initial learning rate of 0.1, which is reduced by a factor of 10 at the 20th and 70th epochs, respectively. The other training configurations are the same as the ones used in Appendix 4. Table 5 shows the performance of five defense methods on the generated poisoned models. From this table, we can find that MCLDef can achieve the best ASR and BA for all the poisoned-label attacks. However, although MCLDef outperforms NC for Sig in terms of both ASR and BA, its defense is not as good

¹<https://github.com/bboylyg/NAD>

²<https://github.com/bolunwang/backdoor>

³<https://github.com/YiZeng623/I-BAU>

Table 4: Performance comparison of five backdoor defense methods on Cifar-10, where data augmentation techniques are not used in the defense.

Attack	Before		FT		NAD		I-BAU		NC		MCLDef	
	ASR	BA	ASR	BA	ASR	BA	ASR	BA	ASR	BA	ASR	BA
BadNets	99.64	83.01	89.96	80.1	49.88	81.73	4.12	79.91	4.62	79.64	2.10	81.81
Trojan	99.38	82.84	98.06	80.49	91.08	81.84	4.32	79.89	4.43	80.69	1.83	82.61
Blend	98.98	84.20	4.47	80.79	14.20	83.03	2.44	82.11	2.93	80.76	1.44	84.89
CL	95.47	86.44	23.21	81.5	22.66	82.18	38.47	82.83	8.42	77.96	0.24	83.57
Sig	99.03	84.64	96.67	80.09	84.32	81.43	75.39	81.27	50.39	71.94	1.66	72.93

Table 5: Performance comparison of five backdoor defense methods on Cifar-10, where data augmentation techniques are used in the training training of poisoned models.

Attack	Before		FT		NAD		I-BAU		NC		MCLDef	
	ASR	BA	ASR	BA	ASR	BA	ASR	BA	ASR	BA	ASR	BA
BadNets	100	89.39	4.93	83.09	9.66	84.81	1.50	85.39	3.10	81.39	0.02	89.01
Trojan	99.78	90.09	3.36	81.69	3.19	83.64	1.61	85.88	2.52	80.97	1.11	87.00
Blend	97.40	89.16	3.24	82.54	4.23	85.04	21.58	85.28	2.81	81.40	2.04	87.06
CL	98.18	90.56	6.40	81.71	7.74	82.90	2.71	86.94	5.77	76.82	0.09	87.79
Sig	97.87	91.06	2.59	82.86	1.04	84.89	1.36	85.80	26.43	68.90	7.92	73.27

as the ones of the other three defense methods (i.e., FT, NAD, I-BAU). Based on the observations in Table 2, the reason for the low performance here is mainly due to the quality of trigger inversion. If a new trigger inversion method with higher quality can be integrated into the first stage, the defense performance of MCLDef will be greatly improved for the Sig attack.

C.2 MCLDef+

As aforementioned in Section 4.4, we find that when the clean data rate exceeds 20%, MCLDef has the best ASR but its BA drops. The main reason for this trend is because the distance between two features within a negative becomes farther along the backdoor purification process. When more and more clean data are involved in backdoor trigger elimination, such mutual exclusion between features imposed by negative pairs will more easily result in the shape change of benign clusters. Therefore, we add an extra stage to verify the phenomenon, named *positive pair correction*. Figure 8 shows an overview of MCLDef+, where stages 1-2 are the same as the ones of MCLDef, while stage 3 tries to further pull the feature representations of poisoned data towards those of their benign counterparts.

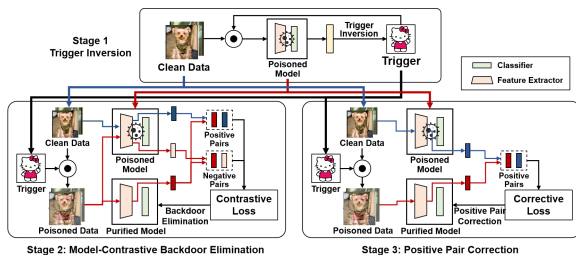


Figure 8: Overview of our MCLDef+ defense method

Assume that \mathcal{D} is a clean dataset with N samples and the trigger obtained in stage 1 is a combination of Δ^* and \mathbf{m}^* . Based on these two things, we can generate a poisoned dataset $\hat{\mathcal{D}}$ by using Equation 1. Let $(\mathbf{x}_i, y_i) \in \mathcal{D}$ be a clean sample and $(\hat{\mathbf{x}}_i, \hat{y}_i) \in \hat{\mathcal{D}}$ be its corresponding poisoned sample. According to the definition of positive pairs in Section 3.4, we can generate the corresponding positive pair (z_i, z_i^{cle}) for \mathbf{x}_i and $\hat{\mathbf{x}}_i$. We define our *corrective loss* for MCLDef+ as follows:

$$\mathcal{L}_{corrective} = \sum_{i=1}^N -sim(z_i, z_i^{cle}), \quad (5)$$

where $sim(\cdot, \cdot)$ represents the similarity of two feature vectors based on the cosine similarity function. In stage 3, we optimize ω as follows:

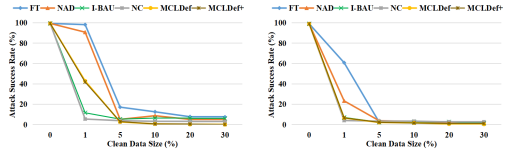
$$\omega^* = \arg \min_{\omega} \mathcal{L}_{corrective}. \quad (6)$$

C.3 Impact of Clean Data Sizes

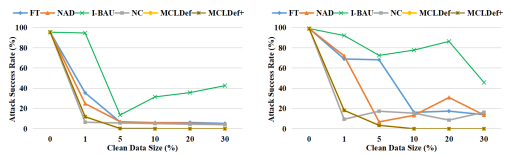
Based on Cifar-10 dataset, Figure 9 compares the defense performance of five defense methods against Trojan, Blend, CL and Sig attacks using different clean data sizes. From this figure, we can draw the same conclusion as the one made in Section 4.4. We can find that more clean data will lead to better ASR, and MCLDef and MCLDef+ can always have the best ASR. Moreover, MCLDef+ can indeed improve the BA of MCLDef.

C.4 Impact of Hyperparameters

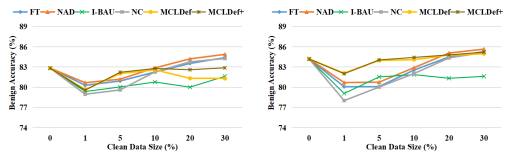
We considered the impact of temperature parameter (i.e., τ in Equation 3) on ASR and BA of MCLDef for the five attack methods. Figure 10 shows the results with different values of τ , where $\tau \in \{0.1, 0.5, 1.0\}$. Note that by default in MCLDef $\tau = 0.5$. From this figure, we can find that a smaller τ will lead to a better ASR, but may result in a notable BA loss.



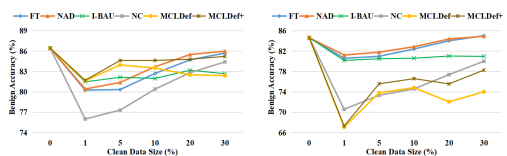
(a) ASR (against Trojan) (b) ASR (against Blend)



(c) ASR (against CL) (d) ASR (against Sig)



(e) BA (against Trojan) (f) BA (against Blend)



(g) BA (against CL) (h) BA (against Sig)

Figure 9: Defense performance of five backdoor elimination methods under different clean data rates.

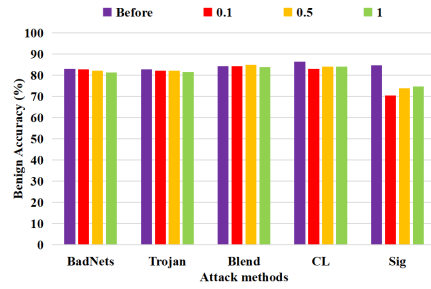
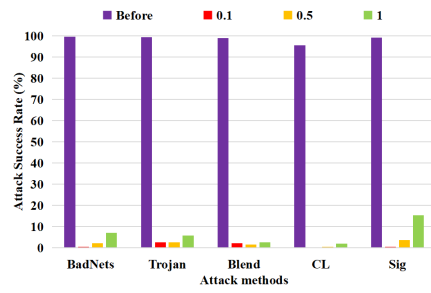


Figure 10: Defense performance of MCLDef on Cifar-10 with different τ .